Supplemental Figure 1.

No significant difference was found in voltage-dependent availability of I_{Na} (**A**) and recovery from inactivation (**B**) between control and CaMKII activating buffer without CaM and CaMKII (vehicle) pipette solutions.

Supplemental Figure 2.

Regulation of I_{Na} gating by CaMKII and PKA. **A.** Steady state availability, **B.** Activation curves, **C.** Recovery from inactivation and **D.** Entry into inactivation in the presence of activated CaMKII and PKA compared with control.

Supplemental Figure 3.

Regulation of peak I_{Na} and the I-V relationship by CaMKII and PKA. **A.** Representative families of currents elicited by the voltage clamp protocol described in figure 2 in control, CaMKII-containing and PKA-containing pipette solutions. **B.** The I-V relationships in the presence of activated CaMKII and PKA compared with control pipette solution. Both CaMKII and PKA increased the peak current densities, PKA further increased the current density compared to CaMKII and shifts the I-V in the hyperpolarizing direction.

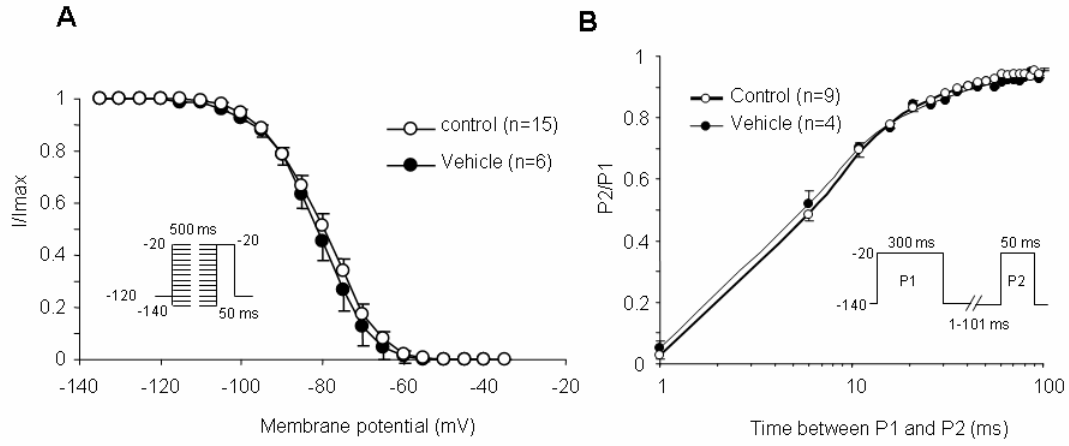

Figure Suppl.1 Aiba T, et al.

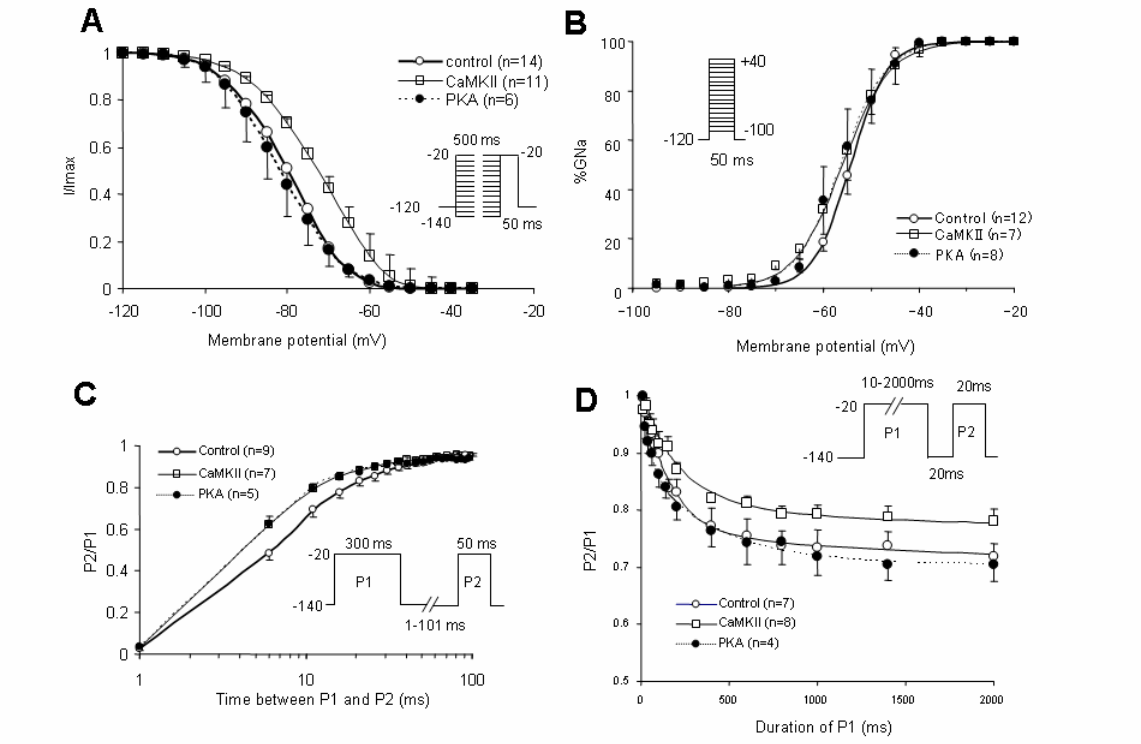

Figure Suppl.2 Aiba T, et al.

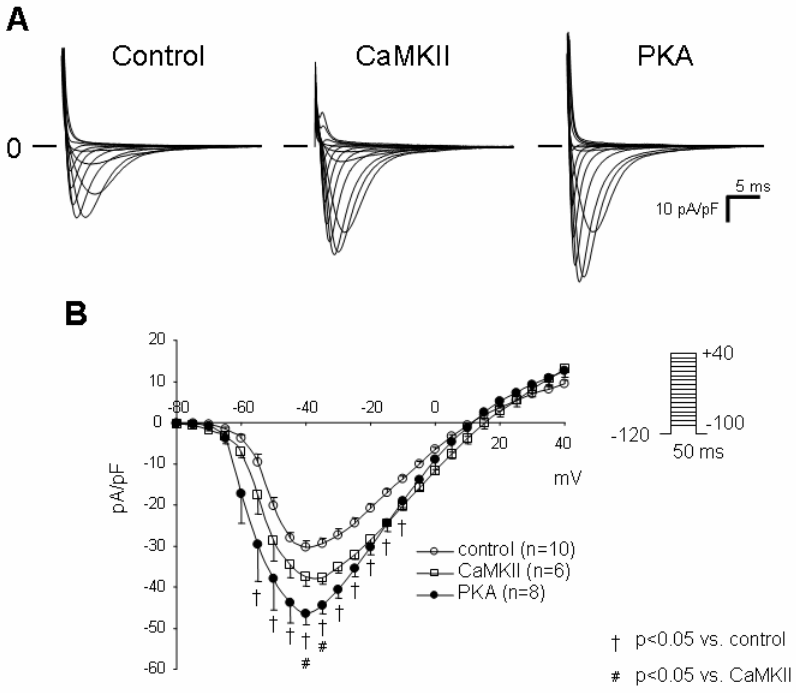

Figure Suppl.3 Aiba T, et al.

Supplemental Table 1

Voltage-dependent Peak Current and Reversal Potential

	Peak current (pA/pF)	Voltage (mV)	Reversal Potential (mV)	n
Control	-30.5 ± 4.7	-40 ± 3	13 ± 4	10
AIP	-31.7 ± 2.2	-42 ± 3	10 ± 4	6
PKI	-33.6 ± 3.6	-39 ± 5	11 ± 5	7
CaMKII	-39.8 ± 6.2 †	-39 ± 4	17 ± 8	6
CaMKII + AIP	-34.0 ± 6.7	-37 ± 8	10 ± 4	7
CaMKII + PKI	-43.4 ± 9.6 †	-41 ± 4	11 ± 2	5
CaM	-41.2 ± 5.0 †	-44 ± 4 †	15 ± 6	6
CaM + AIP	-34.8 ± 4.6	-38 ± 8	9 ± 4	6
CaM + PKI	-39.9 ±9.6 †	-42 ± 5	13 ± 4	6
PKA	-50.7 ± 8.4 †	-44 ± 8	14 ± 8	8

Mean ± SD
† $p<0.05$ vs. control by ANOVA with Bonferroni/Dunn test, Abbreviations are shown in Table 1.